Growth and structure of PbVO₃ thin films

Lane W. Martin,[a)] Qian Zhan, Yuri Suzuki, and R. Ramesh
Department of Materials Science and Engineering, University of California, Berkeley,
Hearst Mining Building, Berkeley, California 94720 and Materials Science Division,
Lawrence Berkeley National Laboratory, Berkeley, California 94720

Miaofang Chi and Nigel Browning
Department of Chemical Engineering and Materials Science, University of California, Davis,
Kemper Hall, Davis, California 95616 and Materials Science and Technology Division,
Lawrence Livermore National Laboratory, Livermore, California 94550

Teruyasu Mizoguchi
Institute of Engineering Innovation, University of Tokyo, Tokyo 113-8656, Japan

Jens Kreisel
Laboratoire des Matériaux et du Génie Physique (CNRS), MINATEC, Grenoble Institue of Technology,
38016 Grenoble Cedex 9, France

Multifunctional materials promise to provide the foundation for a new class of devices in which functional properties are coupled to one another. Examples include magnetoelectric materials in which magnetic and ferroelectric properties are coupled. Here the authors report the successful growth of single phase, fully epitaxial thin films of the multifunctional material, PbVO₃, using pulsed laser deposition. This growth offers an alternative means for the production of PbVO₃ outside of high-temperature and high-pressure techniques through growth of epitaxial thin films on various substrates. The structure of this highly distorted perovskite is examined using x-ray diffraction, Raman spectroscopy, and transmission electron microscopy. © *2007 American Institute of Physics*. [DOI: 10.1063/1.2435944]

Multiferroic materials, in which magnetism and ferroelectricity coexist, have been studied for over half a century and have recently returned to the forefront of materials science. The promise of coupling between magnetic and electronic order parameters and the potential to manipulate one through the other has captured the imagination of researchers worldwide.[1–4] Current research on such materials is focused on a wide range of materials, including single phase materials, with the ultimate goal of obtaining a single phase multiferroic with strong coupling between ferroelectric and magnetic order parameters at room temperature. Single phase multiferroism has been identified in only a few perovskite (ABO_3) oxides including $BiMnO_3$ (Ref. 5) and $BiFeO_3$ (Ref. 6), where the $6s$ electrons of the A-site ion induce ferroelectric properties and the B-site ions control the magnetic properties. Here we examine the material lead vanadate—PbVO₃ (PVO),[7,8] where the $6s$ electrons of Pb induce ferroelectric properties and the V controls the magnetic properties. PVO has been proposed to have antiferromagnetic ordering and a ferroelectric polarization as large as 152 $\mu C/cm^2$ due to large structural distortions in the material.[7–10] To this point, however, the true multifunctional nature of this material is unknown to researchers. Previous studies on PVO (Refs. 7 and 8) focused on high-temperature and high-pressure single crystal growth techniques. Through the use of nonequilibrium thin film deposition techniques, we have been able to stabilize PVO on a number of single crystal substrates and study the crystal structure of this phase.

In the current work, thin films of PVO were synthesized using pulsed laser deposition. Films were grown from a target with nominal stoichiometry $Pb_2V_2O_7$—or the chervetite mineral phase.[11] The growth took place in reducing environments (10^{-6}–10^{-5} Torr of oxygen) at temperatures ranging from 450 to 650 °C. The films studied and reported in this letter were between 50 and 200 nm thick and were grown on LaAlO₃ (LAO) (001). The work on films reported in this letter can be taken to be representative of all the films measured. Additionally, films were grown on LaAlO₃/Si (100), $(La_{0.18}Sr_{0.82})(Al_{0.59}Ta_{0.41})O_3$ (001), NdGaO₃ (110), and SrTiO₃ (001) single crystal substrates, however, here we focus on the films grown on LAO (001) substrates. The films were analyzed using x-ray diffraction (Siemens D5000 four-circle x-ray diffractometer) and were shown to all be 00l oriented, highly crystalline (PVO 002 full-width-at-half-maximum=0.384°), and highly ordered [Fig. 1(a)]. The out-of-plane, c-lattice parameter was determined to be 5.02 Å for all substrates, which is somewhat larger than the value found in the bulk samples of 4.67 Å.[7,8] Additional phi scans enabled us to determine that the PVO films were fully epitaxial with $[100]_f \| [100]_s$ and $[001]_f \| [001]_s$ [Figs. 1(b) and 1(c)], where subscripts indicate film (f) and substrate (s). Channeled and randomly oriented Rutherford backscattering spectrometry (RBS) was additionally used to probe the crystallinity and composition of the PVO thin films. PVO films showed excellent channeling for a lead-based film with a $\chi_{min}=0.15$. The RBS data were fitted using the RUMP software package from Computer Graphics Service and showed that the films exhibited the expected 1:1 Pb:V ratio. Energy dispersive spectroscopy (EDS) was also performed during transmission electron microscopy (TEM) studies to determine the stoichiometry of the material. EDS showed that the majority of samples had a 1:1 Pb:V ratio or were slightly V
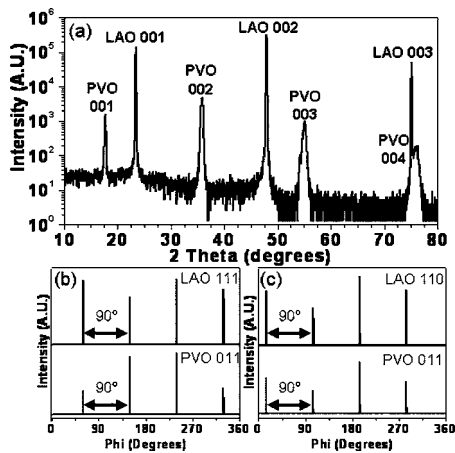
a)Electronic mail: lwmartin@berkeley.edu

FIG. 1. Structural characterization of PVO films on LAO (001) substrates. X-ray diffraction (a) $\theta-2\theta$ showing highly crystalline, epitaxial films of PVO. [(b) and (c)] Phi scans confirming in-plane epitaxial relationships to be $(100)_f\|(100)_s$ and $(010)_f\|(010)_s$.
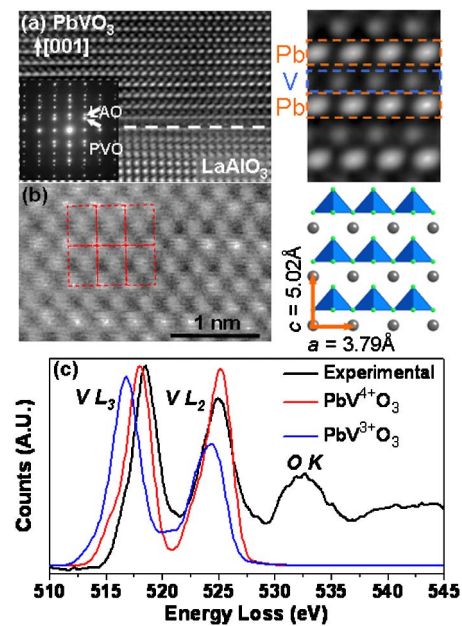

FIG. 2. (Color online) Electron microscopy of PVO films on LAO(001) substrates. (a) Cross-section HRTEM image of the PVO/LAO interface. The inset shows the SAED confirming the in-plane registry of film and substrate. Highly magnified HRTEM image and illustration also illustrate the highly distorted PVO structure. (b) STEM image of PVO down the [010] zone axis. (c) Experimental EELS spectra for PVO along with simulated EELS spectra for V-*L* edge in PVO assuming possible V^{4+} and V^{3+} oxidation states.

rich (Pb$\approx$49.7%, V$\approx$50.3%). This off stoichiometry is to be expected, especially at higher deposition temperatures where the loss of Pb during deposition is likely. These data match well with the RBS data.

Further structural and chemical characterizations were performed using high resolution transmission electron microscopy (HRTEM), selected area electron diffraction (SAED), and scanning transmission electron microscopy (STEM). Cross-sectional HRTEM images taken down the [010] zone axis of PVO [Fig. 2(a)] show a high degree of registry between the LAO substrate and the PVO thin film, as well as the highly distorted nature of the PVO structure. SAED [Fig. 2(a) inset] confirms the in-plane registry between film and substrate and the highly tetragonally distorted PVO lattice. SAED also allows us to determine the in-plane lattice parameter of PVO on LAO(001) substrates to be 3.79 Å, which is perfectly lattice matched to that of the substrate and very close to bulk values from the literature,[7,8] and confirms the out-of-plane lattice parameter to be 5.02 Å. The highly magnified HRTEM image [Fig. 2(a)] and the corresponding schematic illustrate the proposed structure of PVO, showing clear Pb and V rows and the off-center position of V in the tetragonal structure, thus confirming the polar *4 mm* structure found previously.[7,8] Further evidence, through the STEM work is shown in Fig. 2(b). The STEM image gives us a direct picture and confirmation of the true atomic structure of this highly distorted perovskite structure, and once again the proposed structure fits well with the structure seen in this image.

It is important to note that the out-of-plane lattice parameter for the PVO films does not match with that found in the bulk studies.[7,8] We have, however, completed extensive characterization of the structure including both experimental and simulated through-focus series of cross-sectional HRTEM images for the PVO films. The through-focus series was performed over a range of TEM sample thicknesses from 5.7 to 45.5 nm and defocus values from 0 to -80 nm. All simulated images were calculated based on adding an additional distortion to the *c* axis of the unit cell reported in the literature.[7,8] Good agreement is found between contrast and the atomic arrangement in the simulated and experimental images, confirming that PVO has been stabilized in the highly tetragonally distorted perovskite structure with an

even larger *c*/*a* lattice parameter ratio of 1.32 then that reported in the bulk of 1.23.

Additionally, in conjunction with the STEM work, electron energy loss spectroscopy (EELS) was used to investigate the valence of the vanadium ion in PVO by probing the vanadium *L* edge. It is well known that the valence state of the V ion is not the only factor determining the EEL spectra of V-*L* edges and that the crystal structure can also play an important role in determining the spectra.[12,13] Since PVO has a strong tetragonal distortion, it induces one of the two apical oxygen atoms to separate from the normal VO_6 octahedron and causes the formation of corner-shared square pyramids.[7] This arrangement leads to a redistribution of the electrons in this system with more electrons on the V as opposed to the O than is typical in other vanadates with VO_6 octahedrons. This redistribution results in a shift of the energy of the V-*L* edges to the left in the EEL spectra. Additionally, the VO_5 square pyramid structure also induces a different t_{2g}-e_g splitting and therefore affects the fine structures of V-*L* edges. To probe these effects in PVO, the V-*L* edges were modeled using a first principles multielectron method for two cases—PVO with either V^{4+} or V^{3+}, using the experimentally determined structure.[14,15] The experimentally determined and calculated spectra are shown in Fig. 2(d): the energy resolution used for the experimental spectra is $\sim$0.23 eV. It is obvious that the experimental and calculated data match well in both energy shift and the edge shape for the case of V^{4+}. From this work we can say that the vanadium in our PVO films is mostly V^{4+} and we have truly formed the desired d^1 system.

Furthermore, Raman spectroscopy of the PVO film on LAO substrates (Fig. 3) revealed no impurity phases in the PVO films and gave further insight into the structure and quality of the films. In order to understand the observed Raman spectra, comparisons with Raman spectra for similar vanadium-based materials are useful. For instance, CaV_2O_5
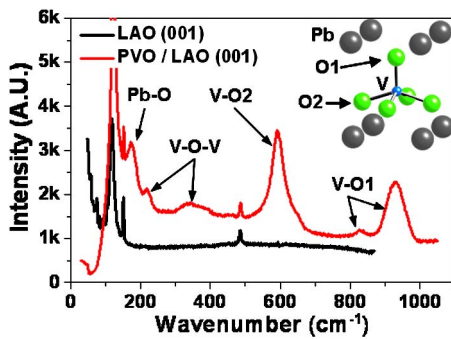
FIG. 3. (Color online) Raman spectra for PVO film on LAO substrate.

is known to have V^{4+} in a VO_5 bipyramid and thus exhibits a similar structure and next nearest neighbor environment to that of PVO. The observation of Raman spectra from $Ca_2V_2O_5$,[16] which displays strong bands at 935 and 638 cm^{-1}, along with the lattice dynamical calculations for NaV_2O_5 (Ref. 17) was used to determine the origin of bands in our PVO spectra. We attribute the observed bands at 830 and 930 cm^{-1} in the PVO films to V−O1 stretching (reflecting the short stiff V−O bond thus a high wave number), the band at 593 cm^{-1} to a V−O2 stretching, and the bands below 500 cm^{-1} to V−O−V bending modes (Fig. 3). Vibrations at wave numbers below 200 cm^{-1} are attributed to vibrations involving the heavy Pb cation as are typically observed in similar perovskites.

Recent density functional electronic structure calculations by Singh[10] predicted that the Raman frequency of the V−O1 bond stretching should lie at 838 cm^{-1}. In agreement with this prediction, we observe a band very close to this value. The assignment of two bands to the V−O1 stretching can be understood by remembering that long range electrostatic forces in a ferroelectric lead to the observation of a LO-TO splitting, as demonstrated by Zhong *et al.*[18] Singh's treatment does not account for this splitting, thus his Raman modes are missing a higher wave number LO band from this bond. As a consequence, we attribute the bands at 830 and 930 cm^{-1}, respectively, to the TO and LO components of the V−O1 bond stretching with A_g symmetry.

Finally, since the initial driving force for investigating this material came under the guise of searching for new multiferroic materials, it is important to note that recent work points to the discovery of multifunctionality in PVO thin films. Experiments using second harmonic generation, x-ray linear dichroism, and piezoforce microscopy have given evi-dence for room temperature piezoelectricity and *G*-type antiferromagnetic order below ∼130 K.[19]

In conclusion, we have grown epitaxial films of PVO on LAO (001) and other single crystal substrates. The structure and chemistry of this highly distorted perovskite material have been investigated in depth and formation of a d^1 system and candidate multiferroic system has been proven. The growth of PVO outside of high-temperature and high-pressure techniques represents a step forward in understanding the chemistry and stability of these new candidate multiferroic films.

[1] N. A. Hill, J. Phys. Chem. B **104**, 6694 (2000).
[2] N. A. Hill and A. Filippetti, J. Magn. Magn. Mater. **242**, 976 (2002).
[3] M. Fiebig, J. Phys. D **38**, R123 (2005).
[4] N. A. Spaldin and M. Fiebig, Science **309**, 391 (2005).
[5] A. M. dos Santos, S. Parashar, A. R. Raju, Y. S. Zhao, A. K. Cheetham, and C. N. R. Rao, Solid State Commun. **122**, 49 (2002).
[6] J. Wang, J. B. Neaton, H. Zheng, V. Nagarajan, S. B. Ogale, B. Liu, D. Viehland, V. Vaithyanathan, D. G. Schlom, U. V. Waghmare, and N. A. Spaldin, K. M. Wuttig, and R. Ramesh, Science **299**, 1719 (2003).
[7] R. V. Shpanchenko, V. V. Chernaya, A. A. Tsirlin, P. S. Chizhov, D. E. Sklovsky, E. V. Antipov, E. P. Khlybov, V. Pomjakushin, A. M. Balagurov, J. E. Medvedeva, E. E. Karl, and C. Geibel, Chem. Mater. **16**, 3267 (2004).
[8] A. A. Belik, M. Azuma, T. Saito, Y. Shimakawa, and M. Takano, Chem. Mater. **17**, 269 (2005).
[9] Y. Uratani, T. Shishidou, F. Ishii, and T. Oguchi, Jpn. J. Appl. Phys., Part 1 **44**, 7130 (2005).
[10] D. J. Singh, Phys. Rev. B **73**, 094102 (2006).
[11] R. D. S. a. C. Calvo, Can. J. Chem. **51**, 70 (1973).
[12] J. H. Paterson and O. L. Krivanek, Ultramicroscopy **32**, 319 (1990).
[13] A. Gloter, V. Serin, C. Turquat, C. Cesari, C. Leroux, and G. Nihoul, Eur. Phys. J. B **22**, 179 (2001).
[14] K. Ogasawara, T. Iwata, Y. Koyama, T. Ishii, I. Tanaka, and H. Adachi, Phys. Rev. B **64**, 115413 (2001).
[15] H. Ikeno, I. Tanaka, Y. Koyama, T. Mizoguchi, and K. Ogasawara, Phys. Rev. B **72**, 075123 (2005).
[16] M. J. Konstantinovic, Z. V. Popovic, M. Isobe, and Y. Ueda, Phys. Rev. B **61**, 15185 (2000).
[17] Z. V. Popovic, M. J. Konstantinovic, R. Gajic, V. Popov, Y. S. Raptis, A. N. Vasil'ev, M. Isobe, and Y. Ueda, Solid State Commun. **110**, 381 (1999).
[18] W. Zhong, R. D. Kingsmith, and D. Vanderbilt, Phys. Rev. Lett. **72**, 3618 (1994).
[19] L. W. Martin, Amit Kumar, Sava Denev, Jeffery B. Kortright, Yuri Suzuki, R. Ramesh, and Venkatraman Gopalan, Phys. Rev. B (to be published).